Available online at www.sciencedirect.com
SciVerse ScienceDirect
Procedia Engineering 59 (2013) 174 – 182
Procedia Engineering
www.elsevier.com/locate/procedia

3rd International Conference on Tissue Engineering, ICTE2013

Spatially multi-functional porous tissue scaffold

AKM Bashirul Khoda[a], Ibrahim T. Ozbolat[b], Bahattin Koc[c]*

[a]*University at Buffalo, Industrial and Systems Engineering, Buffalo, NY 14260, USA*
[b]*University of Iowa, Mechanical and Industrial Engineering, Iowa City, IA 52242, USA*
[c]*Sabanci University, Faculty of Engineering and Naturel Sciences, Istanbul,34956, Turkey*

Abstract

A novel tissue scaffold design technique has been proposed with controllable heterogeneous architecture design suitable for additive manufacturing processes. The proposed layer-based design uses a bi-layer pattern of radial and spiral layer consecutively to generate functionally gradient porosity, which follows the geometric shape of the scaffold. The proposed approach constructs the medial region from the medial axis of each corresponding layer. The radial layers of the scaffold are then generated by connecting the boundaries of the medial region and the layer's outer contour. Gradient porosity is changed between the medial region and the layer's outer contour. Iso-porosity regions are determined by dividing the sub-regions peripherally into pore cells and consecutive iso-porosity curves are generated using the iso-points from those pore cells. The combination of consecutive layers generates the pore cells with desired pore sizes. To ensure the fabrication of the designed scaffolds, the generated contours are optimized for a continuous, interconnected, and smooth deposition path-planning. The proposed methodologies can generate the structure with gradient (linear or non-linear), variational or constant porosity that can provide localized control of variational porosity along the scaffold architecture. The designed porous structures can be fabricated using additive Manufacturing processes.

Selection and peer-review under responsibility of the Centre for Rapid and Sustainable Product Development, Polytechnic Institute of Leiria, Centro Empresarial da Marinha Grande.

Keywords: Multifunctional tissue scafolds; tissue engineering; bioadditive manufacturing.

* Corresponding author. Tel.: +90-216-4839557; fax: +90-216-483-9550.
E-mail address: bahattıinkoc@sabanciuniv.edu

Selection and peer-review under responsibility of the Centre for Rapid and Sustainable Product Development, Polytechnic Institute of Leiria, Centro Empresarial da Marinha Grande
doi:10.1016/j.proeng.2013.05.108

1. Introduction

Reconstructing or repairing tissues with porous structures or scaffolds to restore its mechanical, biological and chemical functions is one of the major tissue engineering strategies. The intended use of such porous structures is to stimulate the tissue regeneration processes while minimally upsetting the delicate equilibrium of the local environment and the patient's biology.

Commonly used tissue scaffold structures are homogeneous in nature with uniform porosity as shown in Figure 1(a). In extrusion based additive manufacturing processes, one of the most common deposition patterns of making porous scaffolds is following a Cartesian layout pattern (00-900) in each layer crisscrossing the scaffold area arbitrarily as shown in Figure 1(a). However, other layout patterns are also reported to determine the influence of pore size and geometry [1]. In such structure, the porosity of designed scaffold do not conform the geometry of the replaced damaged tissue but simply approximates [2]. Besides, jumps or motion without deposition during their fabrication is also highly substantial due to the nature of the tool-path, which is independent of the geometry. And such non-continuous and un-natural movements during fabrication degenerate uniformity of the deposited material shape and need to be avoided [3].

Cells seeded on the scaffold structure need nutrients, proteins, growth factors and waste disposal, which make mass and fluid transport vital to cell survival. However, in traditional homogeneous scaffolds, seeded cells away from the boundary of the scaffold might have limited access to the nutrient and oxygen affecting their survival rate [4]. After cells are seeded in those filaments, their accessibility to the outer region for nutrient or mass transport becomes limited to the alignment of the filament in lieu of their own locations. As shown in Figure 1(a), seeded cells away from the outer contour may have less accessibility through the filament which can be represented by the rectilinear distance. This could affect the cell survival rate significantly as discussed earlier. However, a carefully crafted filament deposition between the outer contour and the medial region can improve the cell accessibility and may increase the mass transportation at any location as shown in Figure 1(b). On the other hand, controlling the size, geometry, orientation, interconnectivity, and surface chemistry of pores and channels could determine the nature of nutrient flow [5]. The size of the pores determines the distance between cells at the initial stages of cultivation and also influences how much space the cells have for 3D self-organization in later stages. Cell seeding on the surface of scaffold and feeding the inner sections are limited when the pores are too small, whereas larger pores affect the stability and its ability to provide physical support for the seeded cells [6].

Natural tissue has a varied arrangement of its micro architecture in concert to perform diverse mechanical, biological and chemical functions. For example, the bone's micro-structure varies considerably making the bone architecture highly anisotropic in nature [7]. But homogeneous scaffolds do not capture the intricate spatial material concentration and may not represent the bio-mimetic structure of the regenerated tissue. A possible solution for performing the diverse functionality would be designing scaffolds with functionally variational porosity. Gradient porosity along the internal scaffold architecture might provide extrinsic and intrinsic properties of functional scaffolds as well as might perform guided tissue regeneration. Thus achieving controllable, continuous, interconnected gradient porosity may lead toward a successful tissue engineering approach. Improved cell seeding and distribution efficiency through the scaffold has been reported in Sobral et al [8] by implementing continuous gradient pore size. Hence the need for a reproducible and fabricatable structure design with controllable gradient porosity is obvious but possibly limited by design and fabrication methods [8, 9].

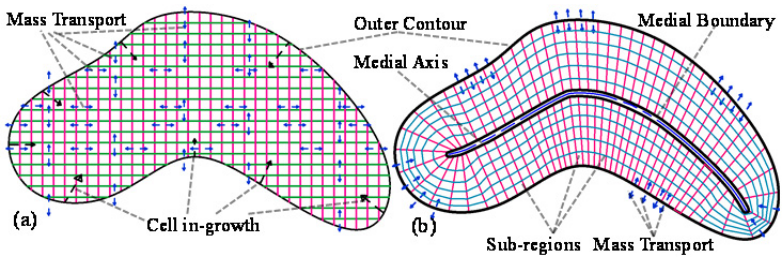

Fig. 1 Mass transport and cell in-growth direction in (a) traditional layout pattern, and (b) proposed radial pattern.

In this paper, we propose a novel method to addresses the scaffold design limitations by designing a functionally gradient variational porosity architecture that conforms to the anatomical shape of the damaged tissue. The proposed layer-based design uses a bi-layer pattern of radial and spiral layers consecutively in 3D to achieve the desired functional porosity. The material deposition is controlled by the scaffold's contour geometry, and this would allow us to control the internal architecture of the designed scaffold. The designed layers have been optimized for a continuous, interconnected, and smooth material deposition path-planning for additive manufacturing processes.

2. Computer-aided bio modeling

The modeling technique has been proposed for layer-based additive manufacturing processes to control the internal architecture of tissue scaffolds. First, the anatomical 3D shape of the targeted region needs to be extracted using non-invasive techniques and layers are generated by slicing the 3D shape. To demonstrate the proposed heterogeneous controllable porosity modeling, two consecutive layers are considered as bi-layer pattern. For each layer, medial axis is constructed as the topological skeleton using inward offsetting method which is then converted into a two dimensional medial region. The scaffolding area is discretized with radial ruling lines by connecting the boundaries of the medial region and the layer's outer contour. An optimization algorithm is developed and sub-regions are accumulated from ruling lines. Dividing the sub-regions into pore-cell along their periphery generates iso-porosity regions for the consecutive layer. The combination of consecutive layers constructs the pore cells with desired pore sizes. Finally, a continuous, interconnected, and smooth deposition path-planning is proposed to ensure the fabrication of the designed scaffolds. By stacking the designed bi-layers consecutively along the building direction will generate the 3D porous scaffold structure with controllable heterogeneous porosity.

2.1. Medial region generation

As mentioned above, the seeded cells away from the peripheral boundary of the scaffold have lower survival rates and tissue formation. In our proposed design processes, the spinal (deepest) region of the scaffold architecture needs to be determined so that the gradient of functional porous structure can change between the outer contour and the spinal region [10]. The medial axis [11] of each layer contour is used as its spine or internal feature.

To ensure the proper physical significance of this one-dimensional geometric feature, a medial region has been constructed from the medial axis for each corresponding layer contour as shown in Figure 2. The medial region has been defined as the sweeping area covered by a circle whose loci of centers are the constructed medial axis. The width of this medial region is determined by the radius of the imaginary circle. Higher width can be used if the scaffold is designed with perfusion bioreactor cell culture [12] consideration to reduce the cell morbidity with proper nutrient and oxygen circulation. The boundary curve of the medial region is defined as the medial boundary in this paper; it is also the deepest region from the boundary, as shown in Figure 2(b). The medial region can be used as an internal perfusion channel through which the cell nutrients and oxygen can be supplied and may increase the cell survival rate.

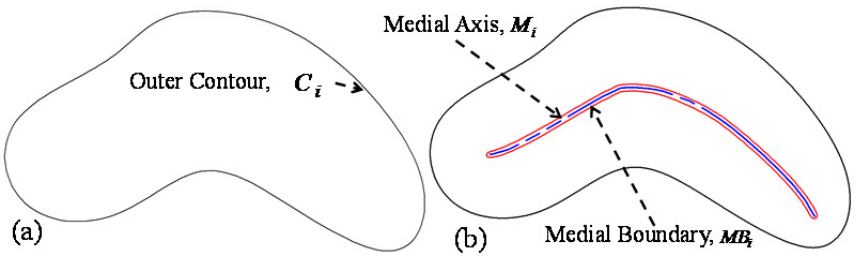

Fig. 2 (a) The layer contour; (b) medial axis, and medial boundary generation.

2.2. Radial sub-regions from generated ruling line

To construct the radial channels or sub-regions, the scaffold area is decomposed into a finite number of segments connected between the external contour $C_i(t)$ and the internal feature $MB_i(t)$. The scaffold area of the i^{th} contour is partitioned with a finite number of radial lines connected between $C_i(t)$ and $MB_i(t)$. To increase accessibility, and to ensure the controllable smooth property transition between the outer and inner contours, an adaptive ruled layer algorithm is developed [10] to discretize the scaffold area with the following conditions:

a) The connecting lines must not intersect with each other.
b) The generated lines must be connected through a single point on $C_i(t)$ and $MB_i(t)$.
c) The line resolution must be higher than the lower width of biologically allowable pore size for cell in growth, ll'.
d) The length of such lines must be the minimum possible.
e) The summation of the inner product of the unit normal vectors at two end points on the contour $C_i(t)$ and the internal boundary $MB_i(t)$ is maximized.
f) The connecting lines must be able to generate a manifold, valid, and untangled surface.

In order to connect both the external contour curve $C_i(t)$ and the internal medial boundary contour $MB_i(t)$, they are parametrically divided into independent number of equal cord length sections. Then, one-to-one point generation methodology [10] is used to generate N number of points on both directrices as shown in Figure 3. Finally, a global optimization model is formulated for ruling line insertion where the objective is to maximize the sum of the function $\frac{\overrightarrow{N(p_{cj})}.\overrightarrow{N(p_{mk})}}{\left|p_{cj}\ p_{mk}\right|^2}$ for all N number of points.

$$Maximize \sum_{j=0}^{N}\sum_{k=0}^{N} \frac{\overrightarrow{N(p_{cj})}.\overrightarrow{N(p_{mk})}}{\left|p_{cj}\ p_{mk}\right|^2} \tag{1}$$

Subject to:

$$LR_s : \{\overline{p_{cj}p_{mk}} \cap C_i(t)\} = \{p_{cj}\} \qquad \forall j,k \tag{2}$$

$$LR_s : \{\overline{p_{cj}p_{mk}} \cap MB_i(t)\} = \{p_{mk}\} \qquad \forall j,k \tag{3}$$

$$LR_s : \{\overline{p_{cj}p_{mk}} \cap LR_{s-1}\} = \varnothing \qquad \forall j,k,s \tag{4}$$

The objective function in Equation (1) considers both unit normal vectors and the distance between the connecting points. During ruling line insertion, they should intersect with the base curve only at one single point $C_i(t)$ and $MB_i(t)$ as shown Equation (2) and (3) to avoid twisting and intersecting ruling lines. Moreover, they should not intersect with each other because intersection generates invalid discretization given in Equation (4). Thus, a scaffold layer is partitioned with N number of ruling line sets $LR = \{lr_n\}_{n=0,1..N}$, and the space between the inserted ruling lines is defined as singular segment sets $LS = \{ls_n\}_{n=0,1..N}$.

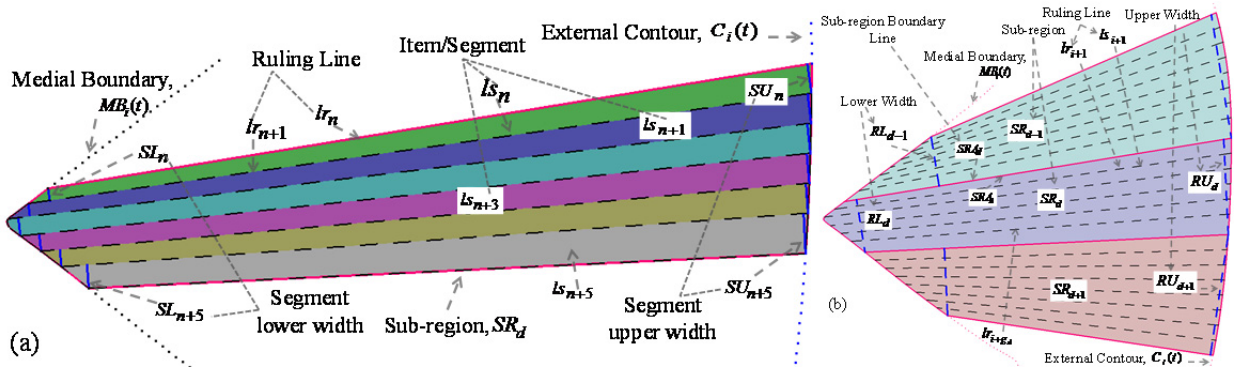

Fig. 3 (a) Sub-region construction from segments, and (b) sub-region's geometry.

By using these segments LS as building blocks, sub-region channels SR need to be constructed by accumulation which will guide the cell in-growth and nutrient/waste flow between the outer contour and the inner region. To ensure the seeded cell in-growth and their support, the geometric properties of these sub-regions must be optimized during the design processes. Thus, the d^{th} accumulated sub-region SR_d is characterized by its area RA_d, lower width RS_d, and upper width RU_d, or as $SR_d = \{RA_d, RL_d, RU_d\}$ $\forall d$ as shown in Figure 5(a). The target values for these variables are defined as RA^*, RL^* and RU^*, respectively, and their values can be determined from the expected pore sizes discussed earlier. An orderly and incremental sub-region accumulation has been performed [10], and the goal is to accumulate the segment sets LS into as few sub-regions SR_d as possible. For uniform geometry, every segment that arrives in the queue may have identical segment i.e. the similar variable values. A set of sub-regions $SR = \{SR_d\}_{d=0,1..D}$, where D is the number of sub-regions, is constructed with a compatible lower and upper width geometry are shown in Figure 4(a).

2.3. Iso-porosity region generation

The generated sub-regions are constructed between $MB_i(t)$ and $C_i(t)$ and act as a channel between them. Their alignment depends upon the outer contour profile as well as the ruling line density. Building a 3D structure by stacking the sub-region layers may be possible; however, this would significantly impede the connectivity within the scaffold area as well as the structural integrity since this may build a solid wall rather than a porous boundary. Since the properties or the functionality of scaffolds are changing towards the inner region, the designed porosity has to follow the shape of the scaffold. Thus iso-porosity regions are introduced which will follow the shape of the scaffold as shown in Figure 4(b). To build the iso-porosity region each sub-region is partitioned according to the porosity with iso-porosity line segments. The porosity has been interpreted into area by modeling the pore cell methodology discussed in our previous work [2].

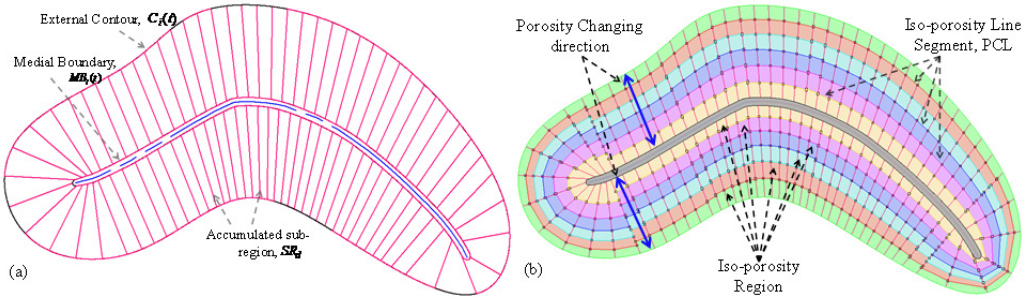

Fig. 4 (a) Discretizing the scaffold area with sub-regions (b) Partitioning the sub-regions by iso-porosity line segments (PCL)

The number of pore cells, $p = 0,1...P$, in each sub-region SR_d depends upon the available area and desired porosity gradient. The number of pore cells need to be the same for all sub-regions to ensure equal number of iso-porosity region across the geometry which will make sure a continuous and interconnected deposition path plan during fabrication. The desired porosity has been interpreted into area and the sub-regions are divided accordingly. The acceptable pore size reported in the literature [13, 14] consider isotropic geometry, i.e., sphere, cube or cylinder. Because of the free-form shape of the outer contour and the accumulation pattern, the generated sub-regions will have anisotropic shapes as shown in Figure 4(b). Thus, the acceptable pore size needs to be calculated from the approximating sphere diameter and can be measured by the following equations. As shown in Figure 4(b), the iso-porosity curve is closed but not smooth and for a better fabrication results iso-porosity curve needs to be smoothed.

3. Optimum deposition path planning

The proposed bi-layer pore design represents the controllable and desired gradient porosity along the scaffold architecture. To ensure the proper additive manufacturing, a feasible tool-path plan needs to be developed that would minimize the deviation between the design and the actual fabricated structure. Even though some earlier research emphasized on the variational porosity design, the fabrication procedure with existing techniques remains a challenge. In this work, a continuous deposition path planning method has been proposed to fabricate the designed scaffold with additive manufacturing techniques ensuring connectivity of the internal channel network. A layer-by-layer deposition is progressed through consecutive layers with zigzag pattern crossing the sub-region boundary line followed by an iso-porosity deposition path planning.

3.1. Deposition-path plan for sub-regions

To generate the designed sub-regions in the i^{th} layer, the tool-path has been planned through the sub-region's boundary lines, and bridging the medial region to generate a continuous material deposition path-plan. Crossing the medial region along the path-plan will provide the structural integrity for the overall scaffold architecture and divide the long medial region channel into smaller pore size. Thus, at first we extended the sub-region's boundary lines towards the medial axis crossing the medial region and then a path-planning algorithm has been developed [15] to generate the continuous path for the sub-region layer fabrication as shown in Figure 5(a). The tool-path needs to start with a sub-region boundary line closest to the end point of the medial axis while starting of the tool-path on another location might increase the number of discontinuities during the deposition process. In addition, if the number of the sub-region's boundary line is odd, then the tool-path should start from the external feature, i.e., from a point on the contour $C_i(t)$, otherwise from a point on the $MB_i(t)$ to reduce or eliminate any possible discontinuity or jumps.

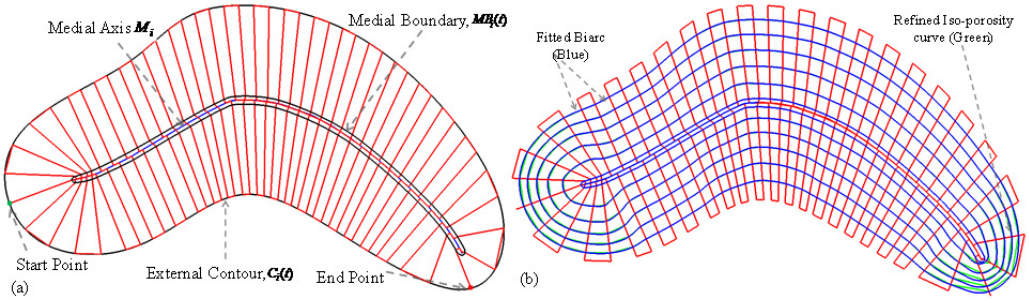

Fig. 5 (a) Decomposing the sub-region's boundary line on the medial axis, and (b) Contrast between refined polygon and fitted biarc

3.2. Deposition path for iso-porosity layer

The iso-porosity curve in the $(i+1)^{th}$ layer can be constructed as a set of piecewise line segments through the inserted cell points as shown in Figure 4(b); however, this can cause discrete deposited filaments because of the stepping and needs to be smoothed for a uniform deposition. Besides, the number of points on the iso-porosity curve requires a large number of tool-path points during fabrication. Linear and circular motion provides better control of the deposition speed along its path precisely for additive manufacturing processes. Thus, a curve-fitting methodology is used to ensure a smooth and continuous path. However, the distribution of cell points may not be suitable for curve fitting techniques, i.e., each sub-region's boundary line contains two adjacent cell points and this can skew curve fitting unexpectedly. Instead, a two-step smoothing for iso-porosity path is proposed [10] to achieve a continuous tool-path suitable for fabrication. In the first step refines the cell point distribution and then a biarc fitting technique is developed to generate C^1 continuity in iso-porosity region path planning as shown in Figure 5(b).

An area weight-based point insertion algorithm has been developed to generate the refined cell points [2]. This will eliminate the stepping issue but could result in over-deposition at the refined cell points because of possible directional changes. A planar iso-porosity curve with C^1 continuity could provide the required smoothness while maintaining the iso-porosity regions. Thus a bi-arc fitting through those refined cell points would be more appropriate for a smooth deposition path. the fitting accuracy of a biarc has been determined based on the one–sided Hausdorff distance [16]. Even though, the biarc has been constructed from the refined point set, the fitting accuracy must be measured from the actual cell point to maintain minimum deviation from the actually computed pore size. The Hausdorff distance provides a robust, simple and computationally acceptable curve-fitting quality measure methodology and can produce a smaller number of biarcs from the cell points.

4. Implementation

The proposed methodologies have been implemented with a 2.3 GHz PC using the Rhino Script and Visual Basic programming languages in the following examples. Two different scripts are written to implement the methodology on bi-layer pattern. The first script starts with the bilayer slice and generates the medial boundary. The second script uses the external and internal feature and generates the final tool-path performing all geometric algorithms sequentially. Time required to execute both script may vary based on the contour shape and desired gradient. However, required time can be reduced significantly by parallel processing or increasing the computational power.

The methodology is implemented on a femur head slice extracted using ITK-Snap 1.6 [17] and Mimics Software [18]. The methodology is implemented for variable but controllable porosity along its architecture. Bio-fabrication of sample models are constructed and fabricated using the micro-nozzle biomaterial deposition system [2]. For visual representation and demonstration purposes, sample models are generated from two consecutive femur slices with larger pore-sizes. A total of 105 sub-regions and three iso-porosity regions are generated with the methodology discussed above. Three sets of controllable porosity, i.e., constant, positive gradient and negative gradient porosity have been designed and fabricated with a 100 micrometer filament diameter as shown in Figure 6.

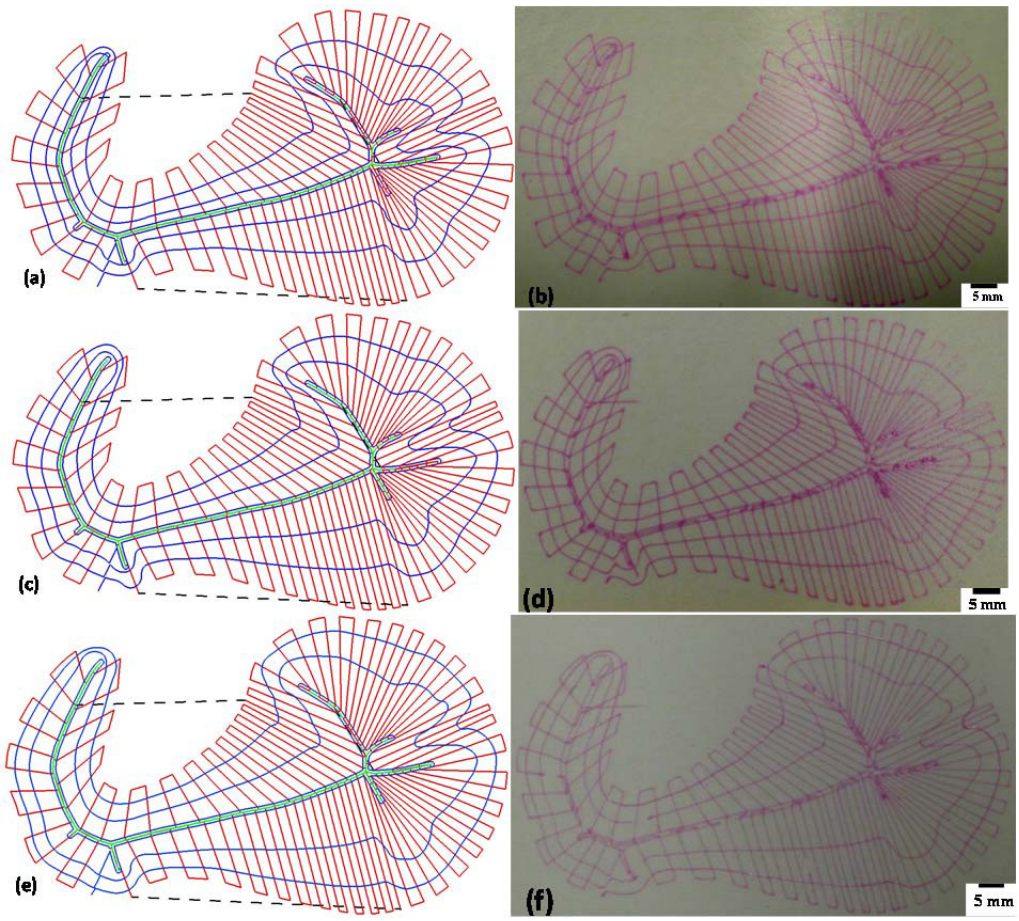

Fig. 6 Model and fabrication for (a-b) decreasing gradient (c-d) constant porosity, and (e-f) increasing gradient.

5. Conclusion

The proposed design algorithm generates the internal points of the designed scaffold sequentially which are supplied to the motion control system to follow the deposition path. The developed methods can be used by any additive manufacturing processes. Heterogeneous or gradient porosity can be achieved through additive manufacturing techniques either by changing the deposited filament diameter or by controlling the segment size i.e., the pore size during the fabrication processes. In this paper, micro nozzle extrusion based additive manufacturing processes are used and controlling of filament diameter may not be possible during deposition process. The fabricated scaffolds could be tested in-vitro and in-vivo with the cells. However, these experiments are beyond the scope of this paper. The mechanical properties, fluid flow dynamics, resolution and accuracy of the fabricated scaffolds may also be used to verify the proposed methodology. However, they are strongly related to the fabrication process used and biomaterials chosen (i.e. viscosity, stiffness), which are out of scope of this paper.

Acknowledgements

The research was partially supported by the EU FP7 Marie Curie Grant #: PCIG09-GA-2011-294088 awarded to Dr. Koc.

Reference

[1] Domingos, M., et al., Evaluation of in vitro degradation of PCL scaffolds fabricated via BioExtrusion – Part 2: Influence of pore size and geometry. Virtual and Physical Prototyping, 2011. 6(3): p. 157-165.
[2] Khoda, A., I.T. Ozbolat, and B. Koc, A functionally gradient variational porosity architecture for hollowed scaffolds fabrication. Biofabrication, 2011. 3(3): p. 1-15.
[3] Khoda, A.K.M.B., I.T. Ozbolat, and B. Koc, Engineered Tissue Scaffolds With Variational Porous Architecture. Journal of Biomechanical Engineering, 2011. 133(1): p. 011001.
[4] Melchels, F.P.W., et al., Effects of the architecture of tissue engineering scaffolds on cell seeding and culturing. Acta Biomaterialia, 2010. 6(11): p. 4208-4217.
[5] Taboas, J.M., et al., Indirect solid free form fabrication of local and global porous, biomimetic and composite 3D polymerceramic scaffolds. Biomaterials, 2003. 24(1): p. 181-194.
[6] Levenberg, S. and R. Langer, Advances in Tissue Engineering, in Current Topics in Developmental Biology, P.S. Gerald, Editor. 2004, Academic Press. p. 113-134.
[7] Podshivalov, L., A. Fischer, and P.Z. Bar-Yoseph, 3D hierarchical geometric modeling and multiscale FE analysis as a base for individualized medical diagnosis of bone structure. Bone, 2011. 48(4): p. 693-703.
[8] Sobral, J.M., et al., Three-dimensional plotted scaffolds with controlled pore size gradients: Effect of scaffold geometry on mechanical performance and cell seeding efficiency. Acta Biomaterialia, 2011. 7(3): p. 1009-1018.
[9] Khoda, A. and B. Koc, Designing Controllable Porosity for Multi-Functional Deformable Tissue Scaffolds. ASME Transactions, Journal of Medical Device (In Press), 2012.
[10] Khoda, A.B., I.T. Ozbolat, and B. Koc, Designing Heterogeneous Porous Tissue Scaffolds for Additive Manufacturing Processes. Journal of Computer Aided Design (CAD) (Accepted with minor revision CAD-D-12-00309), 2013.
[11] Blum, H. and R.N. Nagel, Shape description using weighted symmetric axis features. Pattern Recognition, 1978. 10: p. 167-180.
[12] Gaetani, R., et al., Cardiac tissue engineering using tissue printing technology and human cardiac progenitor cells. Biomaterials, 2012. 33(6): p. 1782-1790.
[13] Karande, T.S., J.L. Ong, and C.M. Agrawal, Diffusion in Musculoskeletal Tissue Engineering Scaffolds: Design Issues Related to Porosity, Permeability, Architecture, and Nutrient Mixing. Annals of Biomedical Engineering, 2004. 32(12): p. 1728-1743.
[14] Hollister, S.J., R.D. Maddox, and J.M. Taboas, Optimal design and fabrication of scaffolds to mimic tissue properties and satisfy biological constraints. Biomaterials, 2002. 23(20): p. 4095-4103.
[15] Khoda, A., I.T. Ozbolat, and B. Koc, Modeling of Variational Gradient Porous Architecture with Multi-directional Filament Deposition in 3D Scaffolds. Journal of Computer Aided Design and Applications, 2013. 10(3): p. 445-459.
[16] Helmut, A. and J.G. Leonidas, Discrete Geometric Shapes: Matching, Interpolation, and Approximation: A Survey, in Technical Report B 96-11, EVL-1996-142. 1996, Institute of Computer Science, Freie Universitat: Berlin.
[17] www.itksnap.org, ITK-SNAP, in 1.6. 2008.
[18] http://www.materialise.com/mimics, Mimics. 2008.